CHEMISTRY IN INDUSTRY

EVALUATION OF PROCESS TRANSIENTS IN GAS COMPRESSION SYSTEMS

AUTHORED BY:

O. P. Armstrong, P. E.

Abqaiq Plants Operations Engineering, Saudi Aramco

ABSTRACT

- The design evaluation of gas compression and flow systems requires careful analysis of flow transients to properly evaluate and predict operational performance of control system and piping system. The methods presented are for electric driven compressors, but can be extended to other types of compressor drivers. The auxiliary systems covered include control valves with PID controller, real pipes, quasi pipes, and heat transfer surfaces. A development of transient or non-steady-state equations is presented. A rigorous non-steady-state model will be valid for steady-state conditions.

- The methods of quantifying these effects involved the use of a generic dynamic simulator program "Vissim". A procedure for determination system startup and operation performance is elaborated for application to trouble shooting designing gas compression systems. The results of the procedure are applied to show how changes in flow and/or temperature impact the operation of a typical system. A series of start-up and operational design questions initiated this evaluation.

EVALUATION OF PROCESS, MECHANICAL, AND CONTROL SYSTEMS TRANSIENTS IN GAS COMPRESSION SYSTEMS

AN EXTENDED ANALYSIS

O. P. Armstrong, P. E.

S. G. Al-Uthman, Process Engineer

Saudi Aramco

Saudi Arabia

Paper P-19,
SECOND INTERNATIONAL CONFERENCE ON CHEMISTRY IN INDUSTRY

Appreciation is given to the
Saudi Arabian Ministry of Petroleum and Mineral Resources and to the
Saudi Arabian Oil Company
for permission to publish this work
And to Saudi Arabian Oil Company staff in review and assistance of this work

SYNOPSIS

Here are some aspects of design optimization and trouble shooting gas compression units. The engineering principles of the method are elicited in an effort to assist others who may be involved in similar systems. Various startup and operational conditions impose constraints on the design of a gas compression system. The key aspects reviewed in this work are: finite element heat balances, thermodynamics of flow and gas compression processes, minimization of flared gas requirements, and optimization of control systems for gas compression. A design case history is given to show how dynamic analysis can be applied to process design.

SUMMARY

Process design is often a dynamic situation where design conditions can change due to operational constraints. During the design phase of a gas compression system a moisture breakthrough test was conducted on the dryer unit to assist in analyzing a persistent problem[1]. The results of the moisture breakthrough test[2] indicated mal-distribution of gas flow among the on-line beds. The flow imbalance was cited as the main causes of premature moisture breakthrough. Both the results of a pressure survey and breakthrough calculations indicated that a single bed was receiving between 70% and 80% of the gas flow. The ideal flow distribution of this system should be 50%. The unit was shut down and substantial blockages caused by pipe scales were removed from the feed distribution piping[3]. The breakthrough testing also indicated that an increase in the on-line time could be achieved due to the moisture loading capacity of the desiccant[2,4]. Subsequently, an extended on-line cycle was initiated[5].

During the course of the initial investigation a differential thermal analysis method was developed to identify requirements of regeneration gas flow rate[4]. The thermal analysis method given here-in is a unique difference equation for calculating thermal cycles of operating plants. Most methods of analyzing desiccant thermal cycles are based on empirical factors for design estimating of equipment sizes and not necessarily applicable to optimizing an operating plant.

This thermal analysis indicated that a substantial decrease in regeneration gas flow rate could be achieved with the extended on-line time. Subsequently the regeneration gas rate was reduced from the design value of 40 mmscfd to a current rate between 23 and 24 mmscfd[5]. This reduction translates into increased gas processing capacity because of decreased recycling of regeneration gas. Present engineering activities are concerned with maintaining a minimum regeneration gas flow rate by optimizing both the thermal and loading cycles.

The current activities underway to optimize these cycles include:
1. Increasing regeneration gas temperature from the current 440F to about 475F. This is to be accomplished with increased condensing pressure of the heating steam. The initial pressure was 440 psig and the final pressure, after re-rating[6] of the steam system, will be 600 psig.
2. Removing slack time from the regeneration cycle pressurization and depressurization steps by increasing orifice sizes and speeding valve opening times.
3. Maximizing performance of gas cooling equipment[7] to reduce water concentration in the dehydrator feed gas. The two items underway in this effort are: Increasing the water rate to allow a decrease the water basin cycles of concentration, thereby minimizing fouling of heat transfer surfaces. Secondly is to remove scale from tube surfaces and maintain maximum fans in service for adequate air flow rate.

BACKGROUND

Molecular sieve drying units are commonly used by industry to reduce the water content of fluids prior to additional processing or as part of product quality control. The two important aspects of zeolite drying materials are the excellent depression of water dew points and the extended life cycle experienced relative to other materials. Another aspect is however that moisture removal processes are more sensitive to the inlet moisture level than are hydrate inhibitor systems. A dehydrator system generally has a total of either 2 or 3 parallel beds[8,9]. The conventional process is a batch operation having one desiccant bed at some phase of the regeneration mode. The math for the conventional process then gives the active beds equal to the total beds less one. This leaves the flow per active bed as the flow divided by the active beds. For 2 bed systems, equal flow distribution does not become an issue when only one bed is on line. With systems of 3 or more total beds, equal flow distribution is essential to smooth operation. For this system there are 3 beds; Beds A, B, and C.

The purpose of this deethanization facility is for improving dew point control in a raw gas transmission line. The line handles a wet sour gas saturated with hydrocarbons at the operating conditions[10]. The deethanization facilities were re-commissioned in the first half of 1993, having been mothballed since the early 1980's. And during the third quarter of 1993 the moisture problems began to occur in this molecular sieve dehydrator unit. Some aspects of this dehydrator unit have been previously published[11].

Figure 1 is a basic process diagram of the system. The sources of the inlet gas are from both NGL stripper overhead gas and K/O drum off gas. Both the K/O drum off gas and the liquids are water saturated during the cooling/condensation cycles prior to the dehydrator. An important aspect is that the combination of stripper overhead gas and K/O drum off gas will be under saturated with water at the feed temperature. The water loading in the gas streams from the stripper overhead gases account for the under saturation. Thus calculation of water rates is more involved over that of a single source feed unit. The water from the stripper gas is based on the water content of liquid hydrocarbon stripper feed. The total water rate being the sum of the K/O drum gas and the stripper feed water. The performance of upstream coolers is a critical aspect of minimizing water rates to the dehydrator.

Another consideration of this system is the high acid gas content of the sour feed gas[12]. Whereas most dehydrator systems have only trace amounts of these components, this feed gas is about 20% acid gases. The H_2S which forms about 1/2 of the total acid gas can either react with oxygen to give elemental sulfur or with CO_2 to give COS. If oxygen intrusion at compressor seals is not minimized then sulfur can reduce desiccant water capacity. If catalytic desiccant materials are installed, excessive amounts of COS will go with the NGL stream. It is required for both oxygen intrusion and COS formation be held at minimum levels.

COS formation is minimized by using a desiccant that is both acid gas resistant and has a minimum catalytic activity toward the COS reaction[13]. The conditions favoring COS formation are increased temperature and low water concentration. After the cooling step of regeneration a thermal gradient exist within the bed and by co-current flow, the coolest section of the dry bed contacts the feed gas to help minimize COS formation.

DISCUSSION

REGENERATION GAS FLOW RATE AND MOISTURE LEVEL

The graphs 1 to 4 detail the impact of various regeneration conditions on the residual water load of typical molecular sieve desiccant. A decrease in the residual water content of a desiccant allows an increase in both the adsorptive and regeneration cycle times. Conversely an increase in residual water content would require a decrease cycle time to avoid moisture breakthrough. The factors which impact the residual water loading capacity of desiccant are; 1) mol fraction of water content in the regeneration gas, 2) regeneration pressure, 3) regeneration temperature.

Graph 1 compares the results of a temperature profile calculation at the bed outlet to actual plant data. The method of analysis is given in the Technical Appendix. The temperature curve for the DC2 gas compares favorably with plant data taken from the B/T test, which shows the time required to reach the maximum temperature ranges between 7 and 8 hours. The variations between the calculated results and plant data at the first hour are thought to result from changes in amount of bed saturation. At the time these data were taken, there was poor flow distribution among the beds. Changing the gas flow rate through the bed changes the amount of unused bed due to changes in the length of the mass transfer zone. The amount of unused bed is what causes the sharp temperature peak at the beginning of regeneration. This is due to water boiling from the fully saturated top and condensing on the bed bottom. The condensation of water releases heat at the bed outlet, spiking the outlet temperature up. This heat at the end of the bed is carried out by the gas over time and the temperature then decreases. Then as the heat wave moves through the bed, the outlet temperature gradually rises again.

Graph 1 was calculated on a basis of 10% dynamic capacity and 25 ppm water in the regen gas at 50 psig regen pressure. The regeneration gas rate was 40 mmscfd with approximately 20% acid gas in almost equal portions of CO_2 and H_2S. The regeneration time for this gas rate was normally considered complete after 8 hours, although after 6 to 7 hours the law of diminishing returns begins to take effect.

Graph 2 is given to show the effect of regen inlet temperature on the outlet temperature profile curve. Again the same sour regen gas from the de-ethanizer overhead was used having the same water conditions as above. However the flow rate has been decreased from 40 mmscfd to only 24 mmscfd. An outlet temperature of 390F occurs after about 9.5 to 10 hours with an inlet temperature of 445F. This agrees with plant practice of 10 hours heating time to yield outlet temperatures ranging between 390F and 405F. However, with an inlet temperature of 475F, the 390F outlet temperature would be achieved in about 7 hours. Hence the objective of increasing the steam pressure on the regen gas heater to increase the regen gas inlet temperature from 445F to 475F.

Graph 3 gives a comparison of regeneration by either fuel gas or deethanizer overhead gas of equal flow rates, pressures, and inlet moisture levels. The key point of this comparison plot is the outlet temperature after at 8 hours. Both gases have about the same outlet temperature and hence, the water loading capacity would be about the same. The calculated dynamic capacity for fuel gas and DC2 gas regeneration at hours 7 and 8 are nearly identical, a difference of 0.1 lb. moisture per 100 lb of desiccant.

The governing condition in the regeneration cycle is the heat rate supplied by the regen gas. The heat rate is the product of the heat capacity and the mass flow rate. Fuel gas has a higher heat capacity than de-ethanizer gas. This virtue offsets most of the molecular weight draw backs of fuel gas. Graph 3 shows both regen gases should require about 8 hours to reach their maximum outlet temperature at a rate of 40 mmscfd. The maximum temperature achieved for DC2 gas is about 5 to 10F higher than fuel gas. This is due to the lower heat rate, (BTU/hr/F) of fuel gas while the wall heat loss rate (BTU/hr) remain nearly constant. The same heat loss (BTU/HR) has a greater impact on fuel gas due to it's lower heat rate. In summary the above graphs show both gases (with identical inlet moisture loadings) have nearly identical regeneration capability at 8 hours. And additional information is necessary to explain the problems encountered with fuel gas regeneration at Abqaiq. Plant practice with fuel gas regeneration required about 50 MMSCFD of fuel gas to get the same performance as with DC2 regen gas. A logical evaluation was to examine the effect of this small temperature difference on desiccant water loadings.

With a regeneration terminal temperature difference of 10F between the two gases, the loading time would be impacted by about 15 minutes per cycle. The major difference in fuel gas and DC2 gas was felt to be the inlet moisture content of the two gases. Changing the water loading from 25 ppm to 200 ppm would decrease the dynamic loading capacity by about 0.7 lb/100lb, as shown by graph 4. This is about a 1.5 hour change in the loading time operation cycle.

What plant measurements confirmed was that placement of a new unit on-line at another plant had increased the water content of the regeneration fuel gas. Prior to the new unit being placed on-line, the fuel gas line typically ran with less than 5 ppm of water. The new pipeline water specifications were increased to 4#/mmscf in winter and 7#/mmscf during summer. This specification translates to between 85 and 147 ppm at pipeline pressure. This translates to a water partial pressure of about 6.9 mmHg. The water content of de-ethanizer offgas is about 6F dew point or 1.3 mmHg.

Based on the graph 4, decreasing the water content of the regeneration gas from 7 mmHg to 1 mmHg would allow the water load on the desiccant to increase by about 1 lb. of water per 100 lb. of desiccant. This would be the equivalent of between 2 and 4 hours extra absorption time for the desiccant beds, depending on the exact water load in the feed gas. The longer time is based on 2250 ppm inlet water for the wet feed gas, with the shorter time being double or 4500 ppm inlet water. By contrast, increasing the regeneration pressure from 50 psig to 100 psig would decrease the absorption cycle by between one-half and one hour, using the above-mentioned wet feed gas water loads. This increase in regeneration pressure could be offset with approximately 40F increase to the regeneration gas temperature.

The impact of the regen gas water load is marginal for one or two year old desiccant, which should have between 24 to 36 hours of on-line time. However as desiccant ages, the on-line time approaches 24 hours. The net impact of wet fuel gas regeneration would be shorter run times before desiccant change-out, when compared to regeneration by de-ethanizer overhead gas.

FLOW RATE VARIATIONS

The results of a three bed Breakthrough test also identified major flow variations within the dehydrator beds. Table 1 documents the extent of these flow distribution problems. The flow distribution problem was identified as the main source of premature moisture breakthrough in the dehydrator beds. The variation of flows is indicated by looking at Table 2, which shows the pressure drops of individual beds, and the breakthrough times of the various beds. Table 2 shows that both Beds B & C experienced extended breakthrough times when Beds B & C ran without being on-line their entire time against Bed A. After fixing the flow distribution problems to beds A and to a lesser extent bed C, then the minimum expected B/T calculates to be 34.2 hours, Table 2.

There were also mitigating circumstances, which compounded the impact of flow distribution problems on premature moisture breakthrough experienced in the plant. The breakthrough capacity of Bed A desiccant was calculated to be 11% (possibly as high as 13% depending on the exact flow distribution). The breakthrough pick-up capacity of Bed B desiccant was calculated to be 11% and the breakthrough pick-up capacity of Bed C desiccant was calculated to be 9.8%. This is compared to an expected water pick-up of between 16% and 18% for new desiccant.

The moisture adsorption capacity was adequate for winter operation without any further modifications. However it was necessary to fix the flow distribution problem. Bed A was found to have a blockage closing about 75% of the pipe diameter on the inlet screen. Bed C inlet pipe screen was found to have about 30% blockage closing of the inlet pipe diameter at the inlet screen. The improvement in flow distribution after blockage removal was ascertained by virtue of the bed pressure drop survey.

COMBINAIRE COOLER EVALUATION[7]

An evaluation was made of the finfan coolers performance during August weather conditions. The performance of finfan coolers is a main factor setting the water loading of the dehydrator feed gas. The finfan coolers used in this application are combined evaporative coolers and air coolers. The water evaporation utilizes the difference between wet bulb and dry bulb

temperatures to improve the cooling efficiency of a conventional air cooler. However the performance of these coolers is largely related to the ambient air relative humidity. For this plant site, the month of August produces the most severe operating conditions on these coolers. The design value of the outlet temperature for either cooler is 115F during August weather conditions.

Graph 5 shows the interstage cooler outlet temperature exceeded the design temperate 15% of the operating days during August 1993. The extreme temperature was 133F for this cooler. Graph 6 shows the performance of the afterstage coolers gave even greater deviations from the design temperatures during August of 1993. For in August of 1993 the outlet temperature was on the order of 150F about 10% of the operating days.

Therefore it can be concluded that the feed gas moisture load during August of 1993 exceeded the design water loading due to higher than expected gas temperatures. The design water loading of the dehydrator is based on a maximum outlet temperature of the gas coolers of 115F. The design temperature would give a water content of the feed gas of about 4200 ppm, while the average water content of the feed gas during B/T testing was calculated to be 2850 ppm, with September temperatures. The feed gas water content during mid summer would be increased substantially over what the beds experienced during B/T testing.

CONCLUSIONS

REGENERATION GAS FLOW RATE AND MOISTURE LEVEL

1. Increasing the water loading of the regen gas will decrease the dynamic water capacity of a desiccant.
2. As decreases are made to the dynamic water capacity moisture breakthrough will occur.
3. The regeneration using fuel gas could at most change the dynamic water capacity by 10%. Since the desiccant charge was relatively new at the time when these problems were experienced, the aging factor would be in excess of the 10% change that could be effected by fuel gas regeneration. Therefore fuel gas regeneration was not a major contributor to the premature moisture breakthrough problems experienced by this dehydrator system.
4. Optimum regeneration gas flow rates change as a desiccant ages.

FLOW RATE VARIATIONS

1. Increased water loading rates can also cause moisture breakthrough.
2. Maldistribution of flow in multiple on-line bed systems can also cause moisture breakthrough.
3. The main source of premature breakthroughs experienced by this system were likely the result of unbalanced flows among the on-line beds.

COMBINAIRE COOLER EVALUATION

1. Increases in feed gas temperature at the location where moisture saturation occurs will bring a corresponding increase in moisture rate to the dehydration unit. These moisture increases can result in premature breakthrough.
2. For this system, the higher than design temperatures from the coolers also made a small contribution to problems during days of extreme temperatures.

RECOMMENDATIONS

1. Benchmark dehydrator performance on a regular basis by breakthrough testing.
2. Adjustments to the on line time should be made based on breakthrough testing results, 90% of breakthrough time is the accepted safety.
3. Based on breakthrough tests, maximize on-line time and reduce regeneration gas rate accordingly.
4. Mitigate finfan performance by cleaning heat exchange surfaces.
5. Mitigate finfan performance by increasing water rate to Combinaire basin for TDS control.
6. Increase regen gas inlet temperature to minimize regeneration gas requirements.
7. Monitor flow distribution among beds on a routine basis.
8. Monitoring the performance of finfan coolers is necessary for smooth operations.

TECHNICAL DISCUSSION APPENDIX

1. DYNAMIC MODEL FOR HEAT EXCHANGE & TEMPERATURES

The typical method presented for calculation of heat exchange temperature profiles uses steady state conditions[14,15,16]. When there is no need for evaluation of control loop performance or transient behavior then the classic design equations are appropriate.[18] The differential equations developed here seek to minimize computational requirements while keeping a good amount of accuracy. A finite difference approach is used to develop the solution. The proposed model will also calculate steady-state performance. This is an initial value problem with boundary conditions. The method uses enthalpy in, less enthalpy out equals accumulation.

The unit volume of heat surface is bounded by a metal volume of $\pi dx \bullet D \bullet dr$. The heat balance on a unit volume, ($\pi dx \bullet D^2/4$), of heat transfer surface, ($\pi dx \bullet D$), leads to the following equations. These heat balance equations will be solved for each segment, dx, over the entire span for each fixed time period, dt:

Considering only sensible heat, the net heat accumulation by unit volume of gas, $A \bullet dx$, inside the tube is (BTU's):

$$dx[\pi/4 \bullet D^2 \bullet \{(\rho \bullet cp)_g\}(T_{to} - T_{to+\Delta t})]_{gas} \quad (1)$$

The net heat absorbed by the surrounding steel (neglecting any radial temperature variations, i.e. infinite thermal conductivity and with inside heat transfer coefficient ≅ than the outside heat coefficient for the unit volume of tube wall is: (BTU's) The net heat lost through the tube wall area, ($\pi Di \bullet dx$, is convected heat. It is determined for the unit volume of gas. This is accomplished by neglecting radial temperature variations. The heat transfer coefficient is the steady state losses applied to the tube inner wall area with overall internal heat transfer coefficient, U (BTU/sec/F/sf),. This value can be calculated from the difference of outlet and inlet temperatures at steady state conditions. The heat lost is based on the average gas temperature less the outside temperature:

$$dx \bullet (\rho \bullet dr \bullet cp)_s \bullet \pi \bullet D \bullet \{(T_{to} - T_{to+\Delta t})_{gas}\} \quad (2)$$

Considering only sensible heat, the net heat release from the flowing gas, (G*A lb/sec) inside a tube is (in BTU's):

$$dt[\{(G \bullet cp)_g \bullet D^2\pi/4\}(T_{xo} - T_{xo+\Delta x})_{gas} - \{\pi \bullet D \bullet dx \bullet (h_{iw}) \bullet (T_{gas} - T_{wall})\}] \quad (3)$$

$$(\pi Di) \bullet dx \bullet (h_{iw}) \bullet dt \bullet [(T_{xo+\Delta x} + T_{xo})/2 - \tau_o]_{gas} \text{ BTU's} \quad (4)$$

The sum of the above heat flows in the gas are equal to the heat gain by the wall and gas. The heat flows above are all positive quantities for a temperature gradient decreasing in the direction of gas flow. Thus the heat lost by the gas must also be a positive quantity and hence the sign of the gas dTx is reversed. Neglecting changes in density & cp over the interval dx, gives:

$$dt[(G\bullet cp)_g \bullet D^2\pi/4\ (\ T_{xo} - T_{xo+\Delta x})_{gas} - (dx\bullet\pi Di)\bullet(h_{iw})\bullet\{(T_{xo+\Delta x} + T_{xo})_{gas}/2 - \tau_o\ \}] \qquad (5)$$

Division of above by $dt(dx)\bullet D^2\pi/4$ and use of the relation $(y_{xo+\Delta x} - y_{xo})/dx \equiv \partial y/\partial x$ gives the net in less out enthalpy:

$$[(G\bullet cp)_g \bullet (-\partial T/\partial x)_{gas} - (4/Di)\bullet(h_{iw})\bullet\{(T)_{gas} - \tau_o\ \}] \qquad (6)$$

The net accumulation of heat is:

$$dx[\{\pi/4\bullet D^2\bullet(\rho\bullet cp\ )_g + (\rho\bullet dr\bullet cp)_S\bullet\pi\bullet D\bullet\ \}\bullet(\ T_{to} - T_{to+\Delta t}\ )_{gas}\ \} \qquad (7)$$

Division of above by $dt(dx)\bullet D^2\pi/4$ and use of the relation $(y_{xo+\Delta x} - y_{xo})/dx \equiv \partial y/\partial x$ gives the accumulated heat in the control volume:

$$\{(\rho\bullet cp\ )_g + (\rho\bullet dr\bullet cp)_S\bullet 4/D\ \}\bullet(-\partial T/\partial t)_g \qquad (8)$$

Using the initial relationship, enthalpy in, less enthalpy out equals accumulation.

$$(G\bullet cp)_g \bullet (-\partial T/\partial x)_g - (4/Di)\bullet(h_{iw})\bullet\{(T)_{gas} - \tau_o\ \} = \{(\rho\bullet cp\ )_g + (\rho\bullet dr\bullet cp)_S\bullet 4/D\ \}\bullet(-\partial T/\partial t)_g \qquad (9)$$

For analysis purposes it is some times helpful to recast the above equation into the partial differential equation format. The final PDE is presented without additional derivation as:

$$\partial T/\partial t = [(G\bullet cp)_g \bullet (-\partial T/\partial x)_g - (4/Di)\bullet(h_{iw})\bullet\{T_{gm} - \tau_o\ \}/\ \{(\rho\bullet cp\ )_g + (\rho\bullet dr\bullet cp)_S\bullet 4/D\ \} \qquad \mathbf{(10)}$$

The validity of the above equation may be verified by evaluation of the steady state equation when $\partial T/\partial t = 0$. to give

$$(G\bullet cp)_g \bullet (\pi D^2\ /4)(-dT_x) \ = \ U(dx)(\pi D\ )(T - \tau_o). \qquad (11)$$

Initial and boundary conditions are important so an analysis of the components to these equations is given to elicit some consideration about the solution method. The term, $(-dT_x)$, equals (Tin - Tout), for the gas and T_{gm} is taken as an average of in and out gas temperatures. The solved temperature is the gas outlet temperature as a function of pipe length and time. The inlet boundary temperature for the gas is the variable inlet temperature. This inlet temperature is calculated based on compressor head and compressor inlet gas properties for a compressor recycle loop. The ambient temperature, τ_o, is taken as a high value, 130F to account for radiant heat flux and to add safety to the calculated values. The initial temperature is taken as equal to the 130F selected ambient temperature. Also the assumption of infinite thermal conductivity requires that metal, gas, and insulation are all equal at any position, x, and time t. Since the thermal mass of insulation would be small compared to the steel pipe wall, the thermal mass of insulation was neglected. The correction factor for finite thermal conductivity is taken up in a decrease of the steel density, or mass. The correct time step must be less than the pipe length

divided by the gas velocity. The following discussion considers some of the alternatives and more about how this solution method was conducted.

Depending on circumstances additional accuracy for the above equation may be required. This can be accomplished by using boundary conditions for the gas limited to the tube wall and solving the boundary wall temperatures by the thermal conduction equations:

$$k[\partial^2T/\partial r^2 + 1/r\ \partial T/\partial r\ ]= (\rho \bullet cp)_S \bullet (-\partial T/\partial t)_S \quad \text{or} \qquad (12)$$

$$k[(\partial T/\partial r|_{ro+\Delta r} + - \partial T/\partial r|_{ro}\ )/\Delta r + 1/r\ \partial T/\partial r\ ] \quad \text{since } hg(Tg - Ts) = k[\partial T/\partial r|_{ro}] \qquad (13)$$

$$[\{k(\partial T/\partial r|_{ro+\Delta r} + - h(Tg - Ts)\ \}/\Delta r + 1/r\ h(Tg - Ts)\ ] = (\rho \bullet cp)_S \bullet (-\partial T/\partial t)_S \qquad (14)$$

Likewise a similar set can be written for the insulation layer conduction

$$\kappa[\partial^2T/\partial r^2 + 1/r\ \partial T/\partial r\ ]= (\rho \bullet cp)_i \bullet (-\partial T/\partial t)_i \quad \text{or} \qquad (15)$$

$$[\{\kappa(\partial T/\partial r|_{ro+\Delta r} + - ho(To - Tis)\ \}/\Delta r + 1/r\ ho(To - Tis)\ ] = (\rho \bullet cp)_i \bullet (-\partial T/\partial t)_i \qquad (16)$$

The term $\partial T/\partial r|_{ro+\Delta r}$ is temperature gradient common to the boundary between the insulation and steel boundary and since they have a common and equal heat flux at the boundary:

$$\kappa(\partial Ti/\partial r|_{ro+\Delta r} = -k(\partial Ts/\partial r|_{ro+\Delta r} \qquad (17)$$

The auxiliary equation, (17) can be solved using the ΔT for the material as a midpoint averaged value. This can be taken as boundary temperature at the known boundaries less the temperature at time for the material, which for the steel is (Tg-Ts) and for the insulation (To-Ti), giving three difference/ differential equations and three unknowns, the gas temperature, the insulation temperature, and the steel temperature to be solved for any time t. The complexity of this method would add substantially to the solution time and requirements on engineering data.

A safe alternative (for heating up calculations) is to take the exterior boundary of the steel as being perfectly insulated, or in math terms, $\partial T/\partial r|_{ro+\Delta r}$= zero. This would eliminate the insulation differential equation set and provide for a safe solution, as heat lost by the insulation would extend the heating time. This solution method is not valid for steady state solution, because at steady state the solution must be gas temperature in equals gas temperature out, an unrealistic solution.

The alternative used was to proceed with the assumption of infinite thermal conductivity with a correction factor to account for real thermal conductivity. This method is presented in various texts. In Kern the method is used for evaluation of regenerator checker brickwork of a blast furnace. The method was considered suitable for calculation of industrial blast furnace and was adapted for this work. For this work an additional safety factor was to neglect the entire steel mass to provide for additional safety.

In the case of very significant changes in gas velocity, the enthalpy term needs to be corrected for the change in velocity head, $(G \bullet A)(V^2)/2gJ$. However most gas process pipe systems are engineered for minimal pressure drop, about .2psi/100'. Also depending on the solution requirements the adiabatic temperature drop across valves may be considered. For the startup gas calculations, the adiabatic valve temperature drop was neglected to provide additional safety to the calculations.

2. SOLUTION FOR GAS/GAS HEAT EXCHANGER TEMPERATURE PROFILES

The gas/gas exchanger solution follows the derivation of Equation10, by using the infinite thermal conductivity assumption and deletion of the momentum energy balance. The resulting equations are two simultaneous differential equations along with one auxiliary equation for LMTD. The thermal masses considered are the steel mass on either shell or tube sides, M_t and M_s. For tube side having steel mass, M, and gas volume, V_t, the accumulation thermal equation is:

$$\partial T/\partial t \bullet \{(\rho \bullet cp \bullet V_t)_g + (M \bullet cp)_S \} \qquad \textbf{(10)}$$

The net exchange of enthalpy with a flow path area of A_t (G*At = mass flow rate) and heat exchange area UA, is:

$$[(G \bullet A_t \bullet cp)_g \bullet (-\partial T)_g - (UA)LMTD] \qquad \textbf{(10)}$$

Completing the equality and solving for the temperature differential equation gives:

$$dT_t/dt = [(G \bullet A_t \bullet cp)_g \bullet (-\partial T)_g - (UA)LMTD]/\{(\rho \bullet cp \bullet V_t)_g + (M \bullet cp)_S \} \qquad \textbf{(10)}$$

An asymmetrical equation for the shell side must be solved simultaneously with the auxiliary equation for LMTD. The inlet temperatures will be fixed and only the outlet temperatures will change with time. The shell side will have a mass composed of shell and internal peripherals plus about 1/2 the tube mass. Shell volume is calculated as internal volume less tube volume, less peripherals mass over steel density. Tube volume is simply internal volume per tube times tube count. For a counter/cross flow exchanger the LMTD is calculated with T for tube temperature and τ for shell temperature,

$$LMTD = F*\{(Ti-\tau o) - (To - \tau i)/ \ln[(Ti-\tau o)/(To - \tau i)]\}$$

The F factor is a thermal factor that depends on exchanger configuration. Many systems are able to use a simpler equation for LMTD:

$$LMTD = F*\{(Ti-\tau o) + (To - \tau i)\}/ 2$$

The maximum time step is based on the minimum gas retention time in either the shell or tube volume, using minimum density. The initial value for the temperatures should avoid temperature crosses, be non zero, and be close to the operating temperature expected to avoid problems with the numerical problems associated with division by zero, infinity or log of a negative number.

3. CALCULATION OF BULK HEAT TRANSFER COEFFICIENTS

The heat transfer coefficients obtained above refer to the rate per square foot of catalyst surface area and apply only between the gas and catalyst surface.

Union Carbide[14] reported that heat transfer resistance occurs in both the gas and catalyst phase for type 5A 1/8" pellets. The overall heat transfer rate is defined as ho and is calculated by:

$$1/ho = (1/h_g + 1/h_S) = (1/h_g + x/k_S) \qquad (25)$$

The solid phase heat transfer coefficient, h_S , is actually the thermal conductivity of the catalyst pellet divided by the average intra pellet heat transfer length, x/k_S.

4. PROOF OF $(T)_{x0+\Delta x\ gas} = (T)_{t0+\Delta t\ cat}$

As was pointed out in the solution of the difference equations, a simplification to the solution was taking the gas temperature as equal to the catalyst temperature after each increment of time. This section is a check on validity of that simplification assumption. The temperature difference between the catalyst and the gas can be estimated by either of 2 approaches[30]. Increasing the heat transfer coefficient decreases the thermal gradient between the gas and the catalyst, i.e. brings the catalyst temperature closer to the gas temperature. Since the value of ho is very large in both cases, the temperature gradient would change very little for these extreme cases.

Calculation of pressure transient

The boundary conditions were taken as follows: inlet mass flow was dependent on the speed of recycle valve closure with an initial spike of 25 mmscfd. The exit pressure was to the inlet of the Abqaiq-Berri gas line at GOSP 6. This boundary condition was considered constant at 450 psig, irrespective of gas flow rate.

The partial differentials were taken as whole differentials because corrections for pipe volume were dropped due to anticipated low pressure changes. The minor pressure changes also provides for the assumption that gas density depends only on pressure, as explained for equation 4, below.

$$\partial G/\partial t = -144g/L\{\Delta(psi) + \Delta G^2/(2\rho g*144) - \Delta p_f\} \quad 1$$

$$\partial \rho/\partial t = \{G_2(t) - G_1\}/L \quad 2$$

Equation 1 calculates the outlet mass velocity out at point 2 given the values of the terms. Equation 2 calculates the upstream pressure transient, given the initial condition of P at the downstream boundary and G at the upstream point. At any given time step the equations are solved for the two unknown values of mass velocity out and the upstream density. The pressure is then calculated from the density by equation 3. The pipe volume is taken as constant, i.e. no elasticity effects on the pipe wall.

$\rho = PM/RTZ$ which can also be arranged to calculate pressure as $P = \rho RTZ/M$ 3a/b

The friction pressure drop is calculated as follows:

$$\Delta p_f = 43.48\{w|w|\}(f*L_e)/\{\rho*d^5\} \quad psi \quad 4$$

Equation 4 uses the time dependent density at the inlet point and the boundary condition flow rate. The frictional pressure loss typically changed from zero to 11 psi as the line was flow packed. The initial pressure was taken at 465 psia and since the pressure loss was less than 10% of the initial pressure, the use of equation 4 is a valid means of determining the pressure drop. The flow was considered isothermal and adiabatic due to the low-pressure drop plus the gas temperature was also approximately ambient temperature.

The friction factor was considered constant and was based on 110% of the fully turbulent value. The approximation was made by equation 5 as given below:

$$f = 1.1*\{1.14 - .86*\ln(\varepsilon/D)\}^{-2} \text{ with } \varepsilon = .000165 \text{ and } D = d/12 \quad 5$$

The solution method for the water hammer differential equations was tested using example problems from V.L. Streeter for liquid water hammer and for damped Utube oscillations. This test was made to verify accuracy the ODE solver. Those results were promising and so the ODE solver was then applied to the above equations.

REFERENCES

1. ARMSTRONG, O.P. '3 Bed Dehydrator Breakthrough Test Procedure Plant 462', APOE/NGL-93-203
2. AL-UTHMAN, S.G. 'Dehydrator Flow Distribution & B/T Time' APOE/ICNGL 93-246
3. AL-UTHMAN, S.G. 'Dehydrator Inlet & Outlet Screens' APOE/ICNGL 93-166
4. ARMSTRONG, O.P. 'Dehydrator Breakthrough Test Analysis Plant 462', APOE/NGL-93-203
5. ARMSTRONG, O.P. '3 Bed Dehydrator On-Line Time Test Procedure Plant 462', APOE/NGL-93-203
6. WALSH, M.P., AL-FAYEZ, A.A. 'Re-rating of Plant 462 Condensate Receiver and Gas Heater', CSD/MCSD/PVVU/L66/94
7. AL-SAYARI, F.S., ARMSTRONG, O.P. 'Hydrojetting Priority 462-E201/202's' APOE/ICNGL 94-099
8. ARMSTRONG, O.P. 'LNG Facilities Design Review', Stone & Webster Engineering Co., Denver Colo. 1985
9. ARMSTRONG, O.P. 'NGL Plants Work Experience', Saudi Arabian Oil Co.., 1988-1994
10. FACILITIES PLANNING DEPT AER-5408. 'ABGG Gas Gathering Study' Saudi Aramco 1990
11. AITANI, A.M., Sour Natural Gas Drying, Hydrocarbon Processing April 1993 p67-73
12. ASHCRAFT, J.A.. 'Plant 462 COS Formation w/Alumina Desiccant, ACU76-64, Dec. 14, 1976
13. JOHN P.T. 'On-Stream Comparison of Grace 564C & UOP SF-1087', APOE 84-234, May 6, 84
14. LUKCHIS, G., M. 'Adsorption Systems', Chemical Engineering 6/11/73
15. BARROW, J.A., Proper Design Saves Energy' Hydrocarbon Proc. Jan. 1983 p117-120
16. GAS PROCESSORS SUPPLIERS ASSN., Engineering Databook 10th ed. 1987 pp20.21-20.24
17. JOHNSTON W.A, 'Design of Bed Adsorption Columns', Chemical Engineering Nov. 27,1972 p. 91
18. ROHSENOW, W.M., HARNETT, JP, 'Handbook of Heat Transfer' McGraw-Hill, 1973, p.18.68
19. RASE, H. F. 'Fixed Bed Reactor Design & Analysis', Chapter 5, Butterworth Publishers, 1990
20. LAITINER H. A., Analytical Chemistry, p515, p.184, Ch.11, 1960, McGraw Hill
21. CARNAHAN B., WILKES J.O., 'Digital Computing & Numerical Methods' Ch.5, p6, Wiley 1973
22. RAMIREZ, W.F., 'Computational Methods for Process Simulations' Ch.8 Butterworth 1989
23. SCHWEITZER, HB of Separation Processes, p3-16, , McGraw Hill, 1979
24. WR GRACE Co., 'Davis Type 3A Molecular Sieves' Product Bulletin
25. UOP Type 4A Molecular Sieves Product Bulletin
26. LUKCHIS, G., M. 'Adsorption Systems', Chemical Engineering , 7/9/73, pp8-12 UOP reprint
27. LUKCHIS, G., M. 'Adsorption Systems', Chemical Engineering 8/6/73 p.14 UOP reprint
28. PORTERFIELD, W. W. 'Concepts of Chemistry', Norton Pub. NYC, 1972 p.607
29. DANIELS, F. ALBERTY, R.A., 'Physical Chemistry' 4th Edition p.8.28, Wiley Publishers 1975
30. SMITH, J. M. 'Chemical Engineering Kinetics', 2nd Ed. 1970, McGraw Hill p.298-300, Ch.10
31. PERRY R.H., Chilton, R.H., 'Chemical Engineers' Handbook' 5th Ed., p.14.6 McGraw-Hill '73
32. MADDOX, ERBAR, 'Gas Conditioning & Processing' Vol.3 1982, Campbell
33. ARISAWA, T. 'Telephone Conversation on O2 Ingression', Saudi Aramco, Oct.19, 1993
34. ATHERTON, DA. 'Telephone Conversation on Plant 462 Dehydrator', 1993
35. VENUTO P. B., HABIB, E. T. 'Fluid Catalytic Cracking with Zeolites' p.47, Dekker 1979
36. POLKOWSKI, G.R., Desiccant Evaluation, Saudi Aramco AIU-Fax & Telephone Conversation, Oct.4, 1993
37. SLOAN, E.D., 'Clathrate Hydrates of Natural Gases' Marcel-Dekker, 1990, p.488 & p.205
38. PARRISH, W.R., PRAUSNITZ, J.M. 'Dissociation Pressures of Gas Hydrates Formed by Gas Mixtures' I&EC Process Design & Development Vol.II, #1, 1976, p.276
39. HUGHES, R., DEUMAGA V, 'Insulation Saves Energy' Chemical Engineering May 27,1974 p. 95-100

GRAPH 1

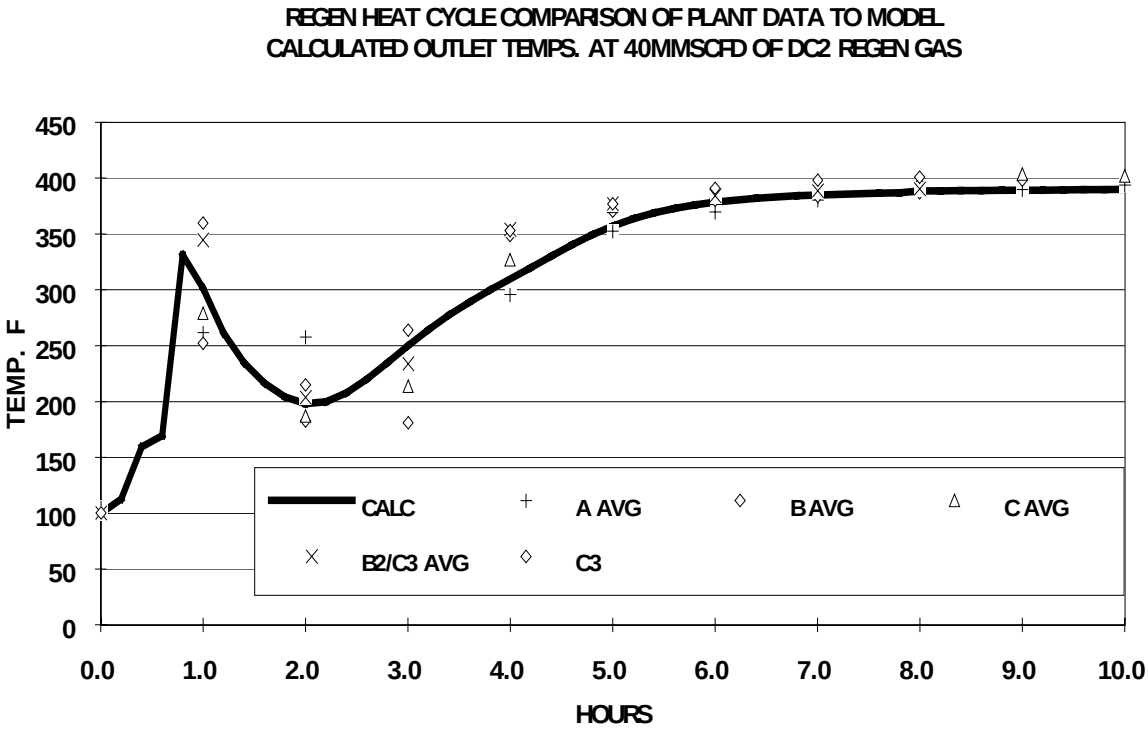

GRAPH 2

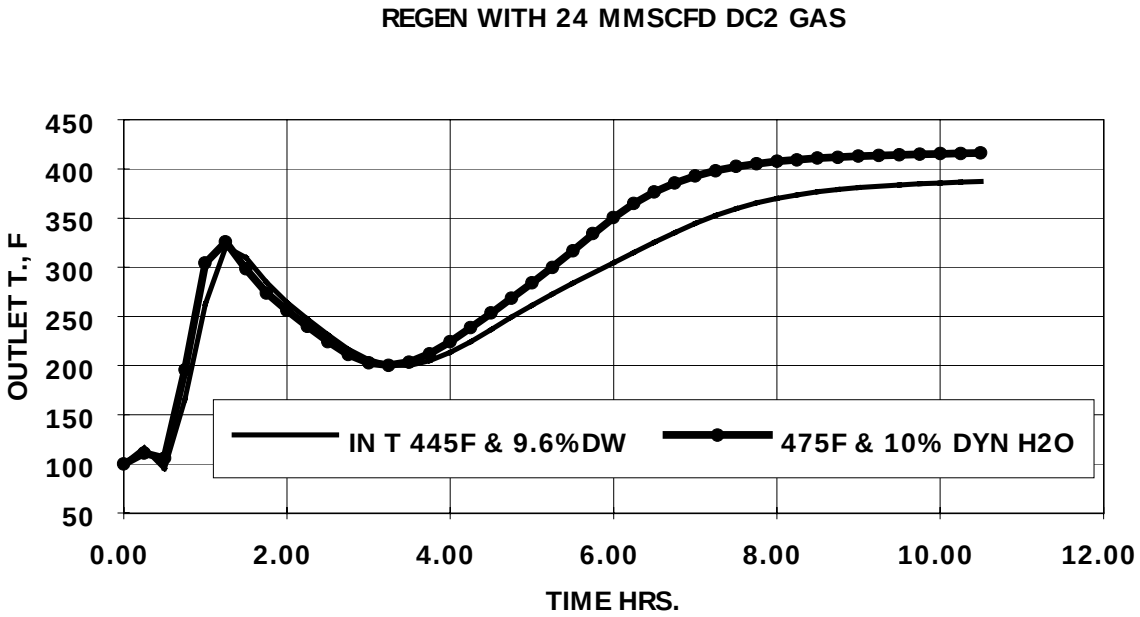

GRAPH 3

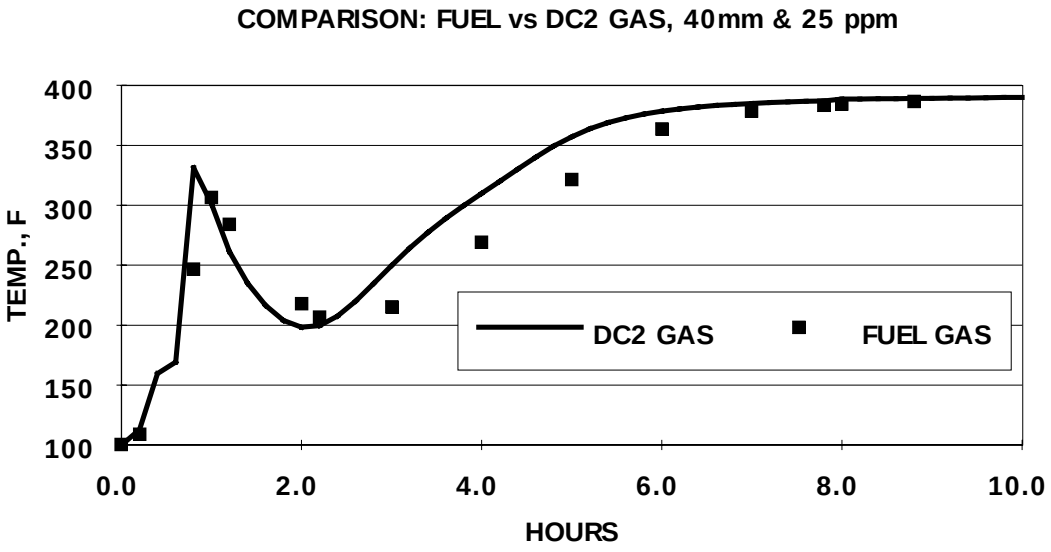

GRAPH 4

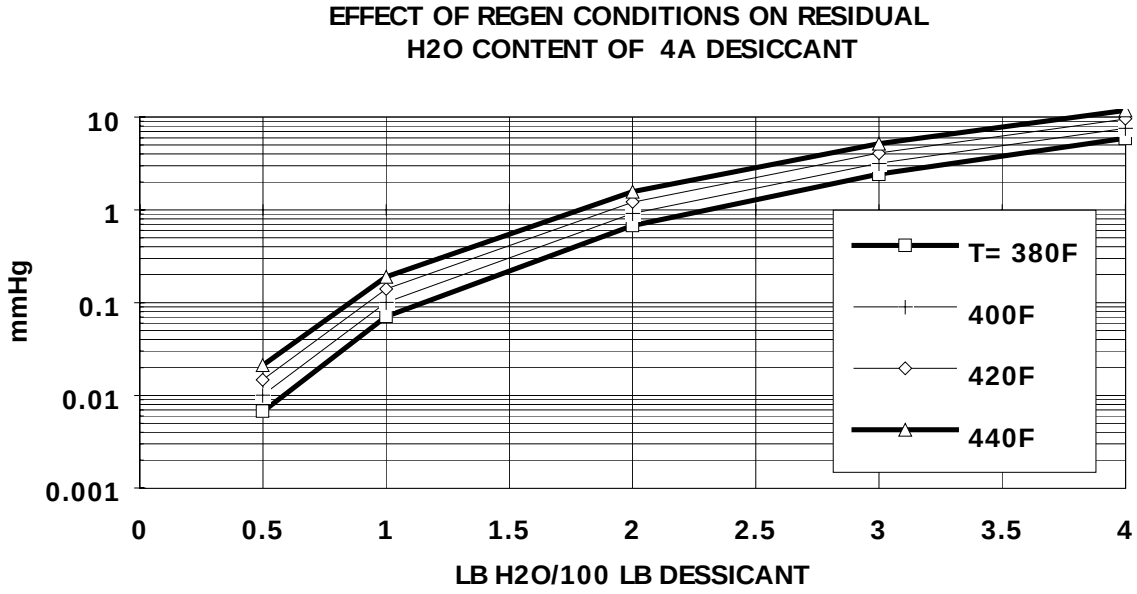

GRAPH 5

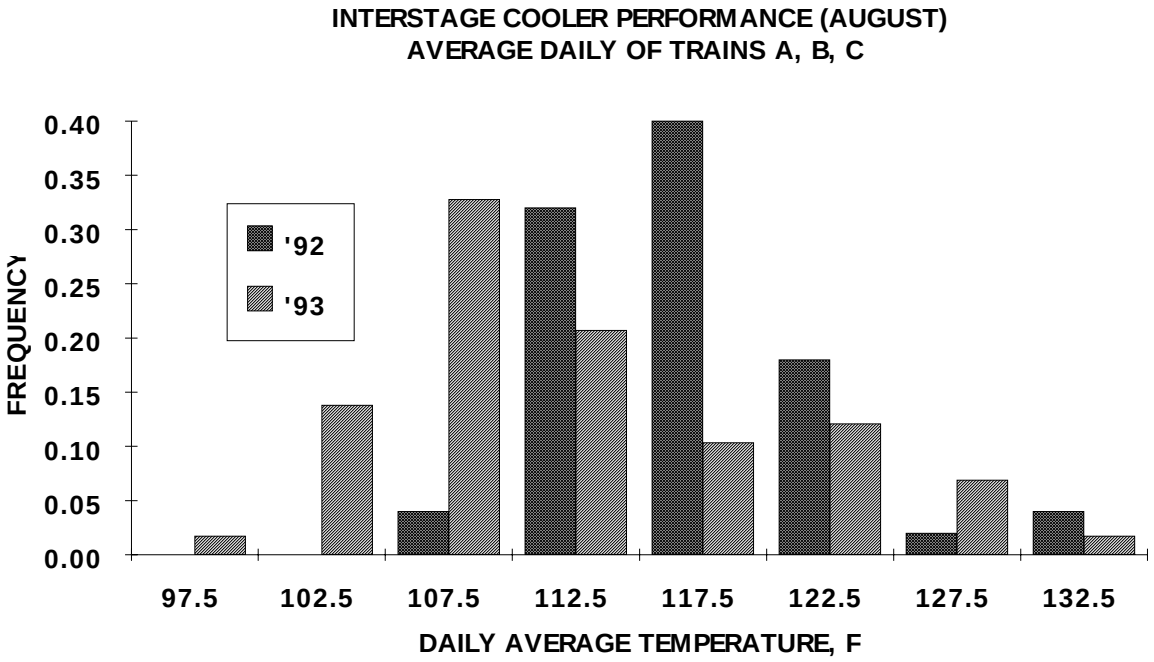

GRAPH 6

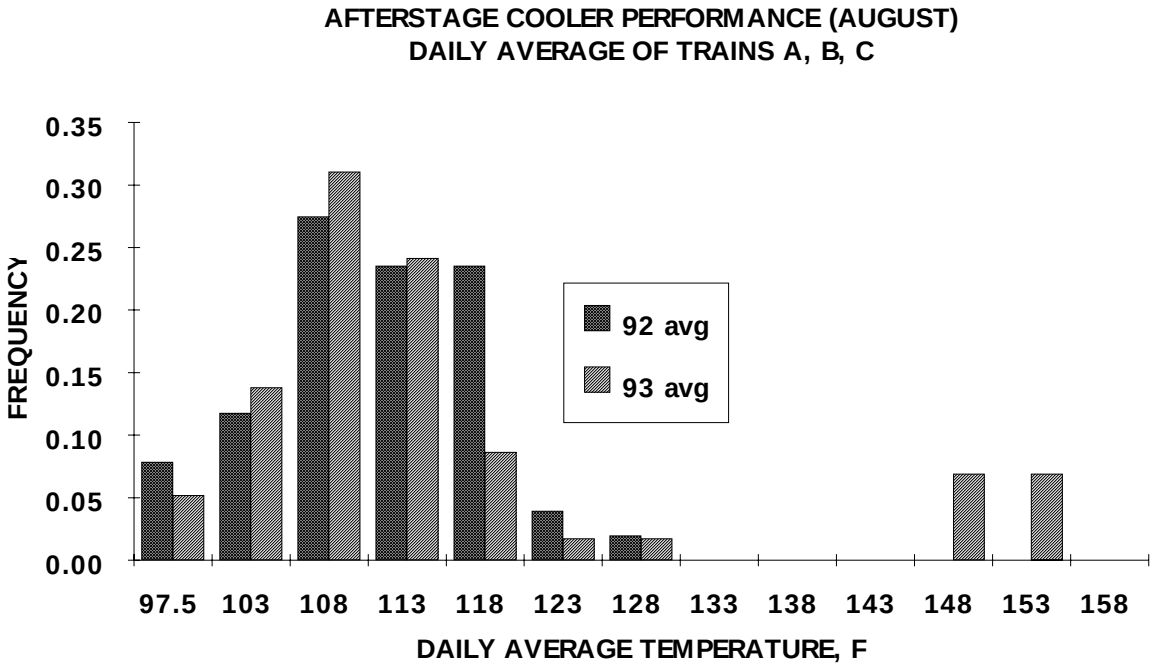

GRAPH 7

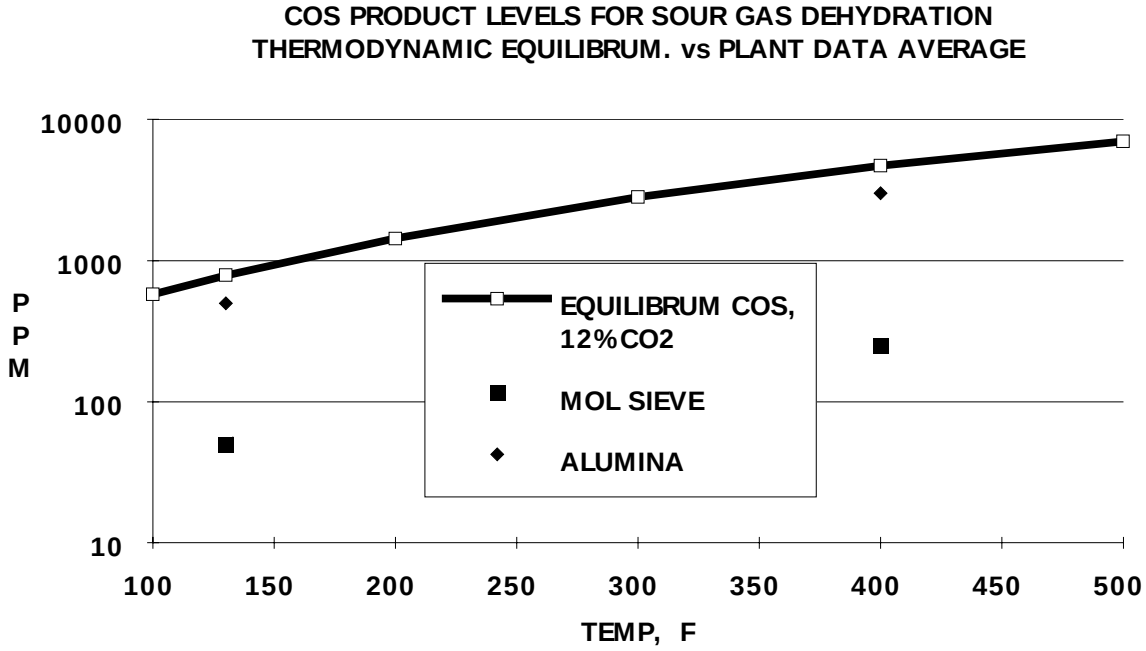

GRAPH 8

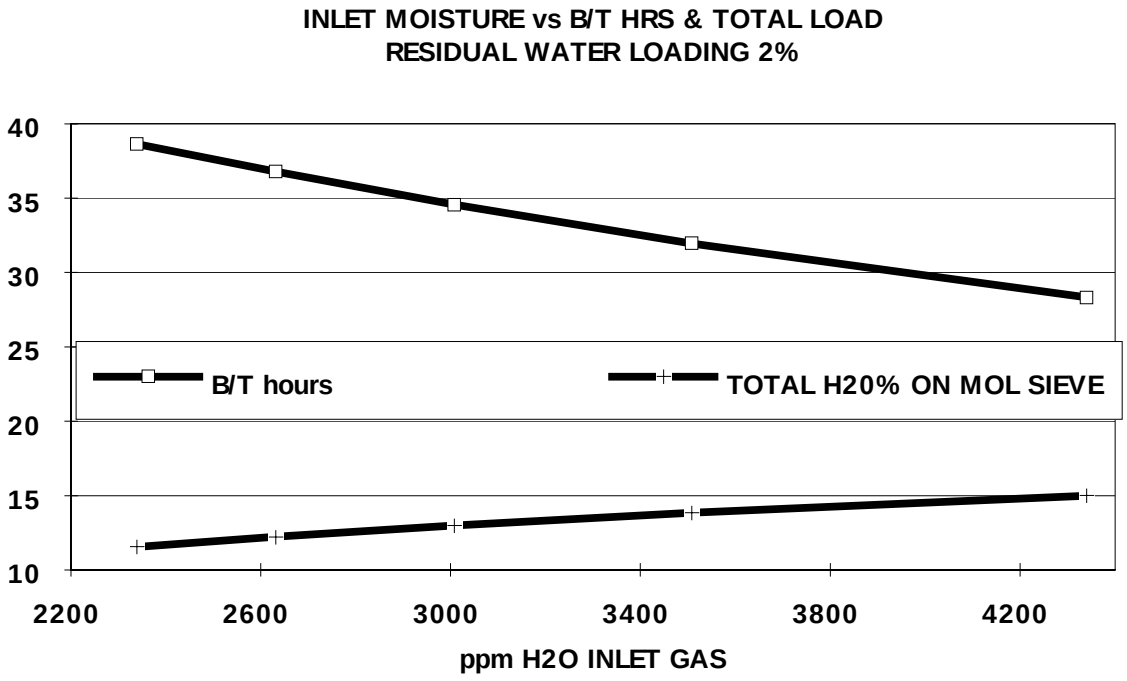

TABLE 1
RESULTS SUMMARY, PRESSURE DROP & FLOW RATIOS

BED	ON LINE WITH	dP PSI	FLOW RATIO %	Remarks
A	B	1	20%	20% of total flow to bed A, when on-line with bed B
A	C	1	30%	30% of total flow to bed A when on-line with bed C
B	A	10.1	80%	80% of total flow to bed B when on-line with bed A
B	C	5.7	61%	61% of total flow to bed B when on line with bed C
C	A	9.94	70%	70% of total flow to bed C when on-line with bed A
C	B	3.68	39%	39% of total flow to bed C when on-line with Bed B

TABLE 2
RESULTS SUMMARY,
BREAKTHROUGH TIMES & DESICCANT CAPACITY

BED	**ON LINE WITH**	**TIME TO B/T**	**B/T H_2O %**	**H_2O PPM AVG.**	**FLOW MMSCFD AVG.**	**EXPECTED B/T TIME ***	**Test Conditions**
A	B & C	80 hr.	10.9	2838	45	39.1 hr*	
B	A	26 hr.	11.0	2903	137	39.6 hr.*	
B	C & A	32 hr.	11.1	2722	120	40.0 hr.*	13 hours w/A, & 19 hrs w/C
C	A	28 hr.	9.8	2829	114	34.6 hr.*	
C	B & A	36 hr.	9.9	2787	89	34.2 hr.*	19 hours w/B & 17 hrs. w/A

*with 90 mmscfd & 2900 ppm H_2O in feed gas

TABLE 3A
SAMPLE CALCULATION

$\{T_{(to+\Delta t)}\} =$
$\{B_g(T)_{xogas} - C_1 + (B_m + B_s)(T_{xocat}) + B_h(t_o - T_{xo}/2_{gas})\}/\{(B_m + B_s) + B_g + B_h/2\}$
Recalling that:
$(B_g) = \{(G \cdot cp \cdot A \cdot dt)_{gas}$, = 1071*.48*122.74*1 = 63098
$(B_s) = (M_s/X) \cdot dx \cdot cp_s$, = 220000/32.6*5.43*.12 = 4397
$(B_h) = (\pi Di) \cdot dx \cdot (h_{iw}) \cdot dt$ = 3.14*12.5*5.43*0.52*1 = 110.9
$(B_m) = A \cdot dx \cdot \rho_c \cdot (cp_c + L_{vxo} cp_w)$, = 122.74*5.43*42*(.22+.1208*1) =9540
$(C_1) = A \cdot dx \cdot \rho_c \cdot [(L_v H_v)_{to+\Delta t} - (L_v H_v)_{to}]_{cat}$ = 122.74*5.43*42*(.1208-.0334)*1575
= 3.85E6
$\{(B_m + B_s) + B_g + B_h/2\}$ = 9540 + 4400 + 63484 + 111/2 = 77146
$\{B_g(T)_{xogas} - C_1 + (B_m + B_s)(T_{xocat}) + B_h(t_o - T_{xo}/2_{gas})\} =$
63098*425 - 3.86E6 + (9540 + 4400)100 + 111(100 - 425/2) = 24.34E6
$\{T_{(xo+\Delta x)}\} = \{T_{(to+\Delta t)}\}$ = (24.4E6) / 77979 = 315.5F

This value being the initial value for the next iteration of temperature at $_{xo+\Delta x}$ and $_{to+\Delta t}$

TABLE 3B

TERM	DEFINITION	EXAMPLE VALUE
gas	gas phase properties and conditions	
cat	catalyst or desiccant phase properties and conditions	
G	regeneration gas mass flux, lb/hr/ft^2	1071
cp	heat capacity, BTU/lb/^{o}F steel =	0.12
	desiccant	0.22
	water	1.0
	gas	0.48
T	temperature, ^{o}F Initial desiccant	100F
	Inlet Gas	425F
ρ	density, lb/ft^3 for the desiccant	42
X	desiccant bed total depth, ft	32.6
dx	desiccant bed increment of depth, ft	5.43
t	the time at which conditions are expressed, hr	
H_V	heat of vaporization, Btu/lb	-1575
L_{vto+dt}	forward water loading , lb of water per lb of desiccant	0.0334
L_{vto}	initial water loading, lb of water per lb of desiccant	0.1208
A	bed cross sectional area sq. ft	122.74
Di	diameter ft.	12.5
dt	forward time difference, hour	1
h_{jw}	overall inside wall heat loss coefficient BTU/hr/sq.ft./F[39]	0.52
M_S	mass of steel, lb.	220,000

TABLE 4
REGRESSION COEFFICIENT VALUES FOR EQN. 18

i	0	1	2	3	4	R	T
a	-908.6	-216.3	35.34	2.28	0.05	1.99/18	460+F
b	0.42	0.62	-0.087	5.2E-3	-1.1E-4	loading is lb H2O	
c	-1604	70.27	-7.24	0.23	1.9E-4	per 100lb sieve	

TABLE 5
EFFECT OF GAS FLOW RATE ON HEAT TRANSFER

GAS RATE MMSCFD	MW	T F	G #/HR/sqft	hg GAS SIDE	ho Overall BTU/cf/F/hr
40	30	440	1071	18177	4073
40	18	440	648	18273	4078
73	30	440	1942	25210	4345
73	18	440	1175	25344	4349
40	30	135	1071	11442	3599
40	18	135	648	12379	3687
73	30	135	1942	15869	3945
73	18	135	1175	17169	4021

TABLE 6
EFFECT OF CO2 & H2S ON WATER LOADINGS

CASE	SPECIES	K	Lgm	GAS mmHg	Li % Total Cap	Conc. ppm	$(KmmHg)_i$
LOW WATER	H_2O	2.5/1	0.23	53.4	11.7	2400	134.00
	CO_2	1/36	0.16	1690	2.9		46.94
	H_2S	1/33	0.16	2667	4.9		80.82
CASE 1	TOTAL				19.5		
HIGH H2O	H_2O	2.5/1	0.23	88.93	14.6	4000	
CASE 2	TOTAL				20.4		

TABLE 7
BASE CASE LOADING STUDY DATA

PARAMETER	UNITS	VALUE
GAS RATE, TOTAL	MMSCFD	170
WATER CONTENT	ppm	4200
WATER RATE/BED	LB/HR/BED	706
DESICCANT CHARGE	LB/BED	168000
ON-LINE BEDS		2
REGEN BEDS		1

TABLE 8
EFFECT OF LOADING ON CYCLE TIMES

	2 BED ADSORPTION		CHANGE IN	
P/U LOAD %	LOAD TIME HR	REGEN TIME HR	O/L TIME HRs per Δ% Load	REGEN TIME HRs per Δ% Load
14%	33.3	16.6		
12%	28.5	14.3	2.4	1.2
10%	23.8	11.9	2.4	1.2
8%	19.0	9.5	2.4	1.2

FIGURE 1